

3D Printing of PolyLactic Acid (PLA) Scaffold Combined with Injectable Bone Substitute (IBS) for Tuberculosis Drug Delivery

Dyah Hikmawati^{1,a*}, Aniek Setya Budiati^{2,b}, Aminatun^{1,c}, Eka Yuliatin^{1,d},
Frazna Parastuti^{3,e}, Prihartini Widiyanti^{4,f}

¹Department of Physics, Faculty of Science and Technology, The University of Airlangga, Surabaya, Indonesia

²Department of Clinical Pharmacy, Faculty of Pharmacy, The University of Airlangga, Surabaya, Indonesia

³Department of Materials Science and Engineering, College of Engineering, National Taiwan University of Science and Technology, Taipei, Taiwan

⁴Biomedical Engineering Study Program, Faculty of Science and Technology, The University of Airlangga, Surabaya, Indonesia

*^adyah-hikmawati@fst.unair.ac.id, ^baniek-s-b@ff.unair.ac.id, ^caminatun@fst.unair.ac.id,
^deka.yuliatin-2017@fst.unair.ac.id, ^efrazna.parastuti-2017@fst.unair.ac.id,
^fprihartini-w@fst.unair.ac.id

Keywords: 3D Printing Scaffold, Injectable Bone Substitute, Drug Delivery, Anti-tuberculosis

Abstract. Spinal tuberculosis is one of the infectious diseases which according to the World Health Organization (WHO), is a major cause of health problems and one of the top 10 causes of death worldwide. The aim of this study was to fabricate a 3D printing scaffold with the design of truncated hexahedron, then combined with Injectable Bone Substitute (IBS) paste as a method for drug delivery in the case of spinal tuberculosis. Injectable Bone Substitute (IBS) paste was synthesized by combining some materials including hydroxyapatite, gelatin, hydroxypropyl methylcellulose (HPMC), and streptomycin. The scaffold was characterized with IBS paste through the digital microscope and the mechanical test to determine the mechanical strength of the scaffold. The results of the 3D printing scaffold showed that the scaffold has interconnectivity between pores. After being injected with IBS, it was seen that the entire surface of the scaffold pores was covered by IBS paste evenly. Scanning Electron Microscope (SEM) tests showed that the surface of the scaffold has been covered by IBS paste, and proves that the pores are still formed. Energy Dispersive X-Ray (EDX) test results showed that the IBS paste containing a hydroxyapatite component consisting of Ca, P, and O elements. Mechanical tests showed that the scaffold for all pore sizes had a compressive strength of 1.49-3.97 MPa before IBS injection and increased to 3.45-4.77 MPa after IBS injection. Then the bending test showed that the scaffold had a bending strength of 16.76-36.09 MPa and increased to around 21.57-40.36 MPa after being injected with IBS. The drug release test showed that the 3D printing scaffold could release streptomycin by 4.944%-6.547%, which has met the percentage of drug release that is able to kill tuberculosis bacteria. It can be concluded that 3D printing scaffold combined with IBS paste can be applied as a drug carrier as well as a method of healing spinal tuberculosis.

1. Introduction

Tuberculosis (TB) is a disease caused by Mycobacterium tuberculosis (MTB). Referring to the [1], 10 million people worldwide suffer from TB and it causes 1.2 million people to die every year. In Indonesia, there were 443,235 TB cases recorded throughout 2021 [2]. In general, TB infects the lungs but can also infect organs such as the spinal. Spinal tuberculosis can cause damage to the vertebral body and spinal deformities that can pose a risk of spinal cord compression [3]. The most effective treatment method that can be used to treat spinal TB is the surgical method, taking the infected bone part and replacing it with a scaffold to induce the spinal stability and healing process [4].

A scaffold is a temporary structure that provides a supportive environment for stem cells to carry out the processes of adhesion, proliferation, and differentiation to produce the desired new bone tissue [5]. In the previous literature, additive manufacturing-based 3D printing attracted attention as a technology that could overcome these drawbacks [6]. The formation of pores and interconnectivity between pores are essential factors in scaffold fabrication [7, 8]. 3D printers based on fused deposition modeling (FDM) have many advantages, such as affordable prices, fast production speeds, and are often used for tissue engineering [9-11]. FDM-based scaffolds have excellent pore interconnectivity to supply nutrients and metabolites required for cell infiltration and cell metabolism [12].

Biodegradable porous scaffolds provide new approaches methods to orthopedic surgery to repair bone injuries [13]. Biodegradable polymers are one of the most commonly used 3D printing materials due to their favorable physiochemical properties. In previous research, several polymers, such as PolyLactic Acid (PLA), Polycaprolactone (PCL), and Poly Lacticco-Glycolic Acid (PLGA), have been reported on the fabrication of bone tissue engineering scaffolds through different 3D printing techniques [14-17]. Among biodegradable polymers, PLA is one of the most important biopolymers with its substantial application in the field of medicine, such as for bone tissue engineering, medical implants, drug delivery system, bone fixation and reconstruction, and suture material [18,19].

Besides being used as a place for cell growth, the scaffold can also function as a drug carrier. The scaffold is filled with Injectable Bone Substitute (IBS) paste which consists of Hydroxyapatite (HA), gelatin, Hydroxy Propyl Methyl Cellulose (HPMC) and streptomycin [20]. Hydroxyapatite is the main portion of the extracellular matrix consisting about 60-70% of the bone mass [21]. It is generally used as a macroporous ceramic for healing bone tissue [22]. Hydroxyapatite is extensively used in various biomedical applications (gene therapy, drug delivery system, regenerative medicine, and tissue engineering) due to its excellent biocompatibility, osteoconductivity, bioactivity, and chemical stability [23-27]. However, hydroxyapatite has the disadvantage that it is brittle, so it needs to be combined with other materials to form composites, especially gelatin. Gelatin is also biocompatible, biodegradable, non-toxic, and is often used in medicine. Due to its hydrophilicity, gelatin has great affinity with HA and shaping through the gel which has perfect combination with the HA [28]. HPMC is used as a gelling agent while streptomycin is a drug that can help the healing process in case of spinal tuberculosis [29].

The mechanical properties of the scaffold should be similar to the mechanical properties of the natural bone at the defect site to ensure the implant is providing sufficient support [30, 31]. Larger pores favor high vascularity, but an increase in cavity volume decreases the mechanical strength of the scaffold [32]. In conclusion, this study aims to fabricate a 3D printing scaffold with the design of truncated hexahedron, combine it with an IBS paste, and then applied as a treatment of spinal tuberculosis. SEM-EDX test was conducted to observe the surface of the scaffold after IBS paste was injected, and to determine the percentage of elemental composition on the scaffold. Mechanical tests, including compressive and bending test, was conducted to determine the mechanical strength of the scaffold so that it can be qualified with the characteristics of human bones. A drug degradation test was also conducted to determine the level of streptomycin released from the scaffold. The contribution of this study is that the pore size and the pore design of 3D printing scaffold can be used as an alternative as a drug delivery that is possible with various doses of drug depending on the severity of tuberculosis cases or bone osteoporosis. The 3D printing scaffold design can be made according to the shape and architecture that can cover bone defects which can be adjusted according to the results of the radiography.

2. Materials and Methods

2.1 Materials

PolyLactic Acid (PLA) filament was used as the main scaffold material, IBS paste ingredients including hydroxyapatite powder from cattle bone comes from hospital tissue bank dr. Soetomo, Surabaya, Indonesia, aquades, gelatin (150 bloom Rousselot, Guangdong, China) from cowhide, Hydroxy Propyl Methyl Cellulose (HPMC) (Sigma Aldrich H7509, Singapore), and streptomycin sulfate from PT. Meiji Indonesia. The material for the drug release test was Phosphate Buffer Saline (PBS) with a PH of 7.2 from maxlab, Tangerang, Indonesia.

2.2 Methods

At first, In the 3D printing scaffold fabrication, the scaffold design uses the SolidWorks 2014 software with a truncated hexahedron-shaped unit cell with a 2 mm width. The process of the design begins by making octagon shapes on the front, top, and right. Then flipping the planes at an angle of 90^0 , so the design framework is obtained. All of the sides were swept using Swept Boss/Base, so a truncated hexahedron unit cell is obtained. The test samples were designed according to the standard with various pore sizes of: 600, 800, 1000, 1200, and 1400 μm . The pore size was made by determining the distance between the fibers (strut). The process of merging or assembly is carried out on the unit cell to obtain a geometric design. The design results of the SolidWorks 2014 application are saved in *.stl* format. The scaffold was printed using a 3D printing machine based on the FDM method with a nozzle diameter of 0.4 mm.

The next step is the synthesis of IBS paste was carried out according to the research [4]. The gelatin solution (20% w/v) was stirred for 1 hour at 40^0C , then the synthesized hydroxyapatite with the composition of HA: gelatin (65:35 w/w) was added. Streptomycin (10%) was added to the solution. In the last step, the HPMC solution was added to the mixture at a temperature of 40^0C for 6 hours.

In the scaffold characterization, several tests were carried out. Scaffold pore observation was carried out using a digital microscope. The surface morphology of the scaffold after injection of the IBS paste was observed using SEM test, while the determination of the percentage of elemental components was conducted using EDX test. The mechanical strength of the scaffold was obtained through compressive and bending tests on the scaffold before and after IBS injection.

The compressive strength is calculated using Equation 1. Where F is the magnitude of the applied force (N), while A is the initial cross-sectional surface area of the scaffold (m^2).

$$\sigma = \frac{F}{A} \quad (1)$$

The equation for calculating the bending strength value can be seen in Equation 2. F is the amount of force applied (N), L is the length of the scaffold (m), b is the width of the scaffold (m), and d is the thickness of the scaffold (m).

$$\sigma_s = \frac{3FL}{2bd^2} \quad (2)$$

A drug release test was conducted to determine the amount of streptomycin released from the scaffold. Scaffold injected with IBS was immersed in Phospate Butane Saline (PBS) solution, then tested in a UV-Vis spectrophotometer to specify the concentration of streptomycin.

3. Results and Discussion

3.1 3D Printing Scaffold

One of the results (pore sizes of 1000 μm) of a 3D printing scaffold with a geometric design of the truncated hexahedron can be seen in Figure 1. It can be seen that the printed scaffold has interconnectivity between pores. After IBS paste was injected, it can be seen that the entire surface of the 3D scaffold pores was covered by IBS evenly.



Figure 1. (a) 3D printing scaffold design, (b) result of 3D printing scaffold, (c) 3D printing scaffold injected with IBS paste

3.2 Injectable Bone Substitute (IBS) Paste

The results of the IBS paste synthesis appear white based on the main ingredient, namely hydroxyapatite. Characterization in the form of FTIR test results, injectability, setting time, acidity and cytotoxicity can be referred to in research [4]. The results of IBS paste synthesis can be seen in Figure 2:

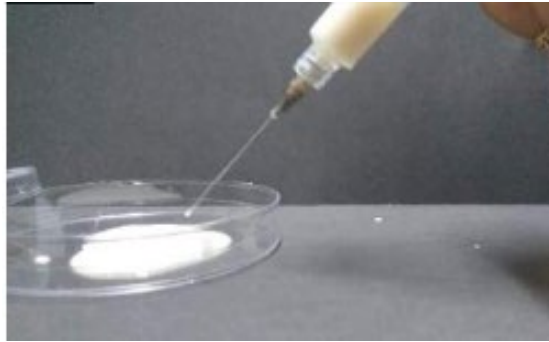
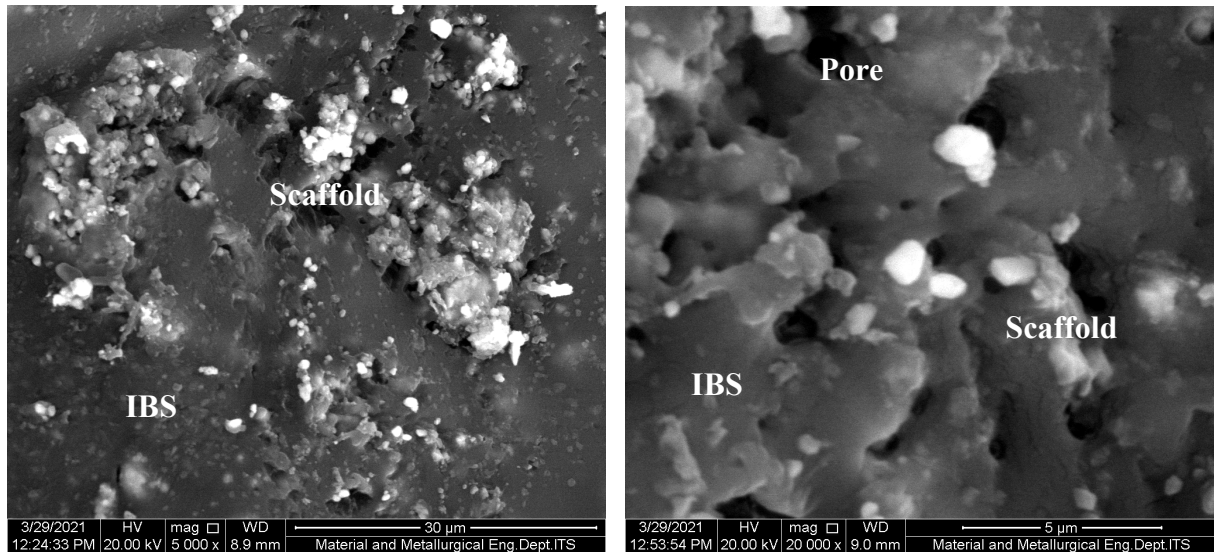


Figure 2. IBS paste synthesis result

3.3 SEM Test

SEM test was carried out with magnifications of 5000x and 20000x on scaffolds with a pore size of 600 μm which showed that the surface of the scaffold had been covered with IBS paste, and proved that there were still pores formed. The pore results seen in the SEM test results are smaller than the digital microscope results, this can be caused by the selected surface is not exactly the same between the two tests, with the surface not clearly visible in the SEM test results. In addition, on the surface of the scaffold there are dots that represent hydroxyapatite crystals from IBS [4]. This is based on the fact that the HA material used in the synthesis of the IBS paste is not a nanoparticle, so there are still white dots in the form of a granular which indicates HA crystals. The results of SEM tests on the surface of the scaffold can be seen in Figure 3:



(a)

(b)

Figure 3. SEM test results for scaffold after IBS paste injection (a) 5000x magnification (b) 20000x magnification

3.4 EDX Test

The presence of hydroxyapatite and other compositions in the 3D printing scaffold injected with IBS paste was shown by the EDX results. The results of percentage of elemental composition can be seen in Table 1, and then the graph results of EDX analysis was shown in Figure 4:

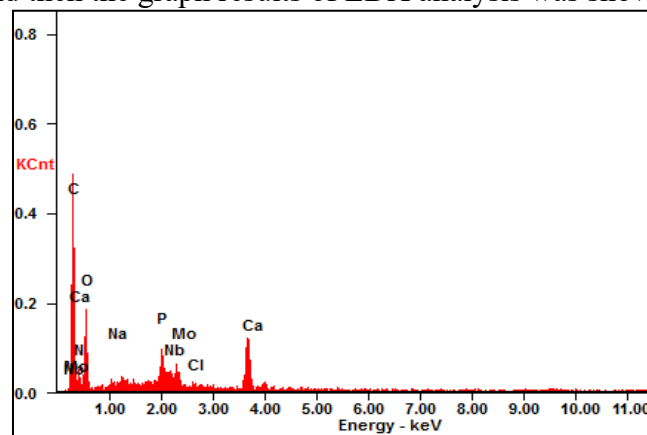


Figure 4. EDX analysis for scaffold after IBS paste injection

Table 1. Percentage of elemental components

<i>Element</i>	<i>Wt%</i>	<i>At%</i>
<i>CK</i>	37.47	50.68
<i>NK</i>	09.84	11.42
<i>OK</i>	29.02	29.46
<i>NaK</i>	01.62	01.15
<i>PK</i>	03.88	02.04
<i>NbL</i>	05.11	00.89
<i>MoL</i>	04.09	00.69
<i>ClK</i>	00.83	00.38
<i>CaK</i>	08.13	03.29

EDX results showed that in the IBS paste there was hydroxyapatite powder consisting of Ca, P, and O elements. P in hydroxyapatite is 1.67 [33]. The Ca/P ratio which is greater than the

theoretical value indicates that the calcium content in HA is greater than the phosphate content. There are also other elements which observed as impurity elements. It may come from the initial material, or are caused by an unsterile manufacturing process.

3.5 Compressive Strength

The results of the compressive test on the scaffold can be seen in Figure 5. Based on Figure 5, it shows that the pore size affects the compressive strength of the scaffold. The increase in pore size causes a decrease in the compressive strength of the scaffold. The addition of IBS paste into the scaffold also affects the compressive strength value. The value of the compressive strength of the scaffold will increase after being injected with IBS paste. The value of the spine compressive strength is 1.5-7.8 MPa [34], so based on these results, the compressive strength value of each scaffold meets the criteria as a bone substitute.

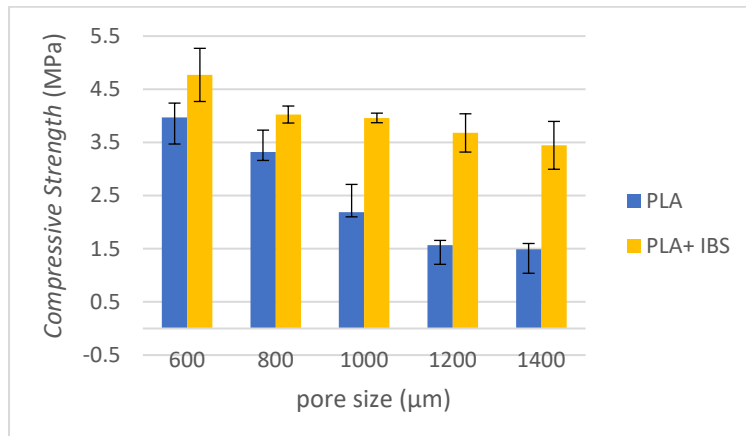


Figure 5. The graph of the compressive strength test results of PLA and PLA+IBS scaffolds

3.6 Bending Strength

The results of the bending test for scaffolds before and after IBS injection can be observed in Figure 6. Based on Figure 6, there is a negative relationship between the pore size of the scaffold and the bending strength value for both scaffolds without IBS injection and after IBS paste injection. The addition of IBS paste into the scaffold increased the bending strength value. This was due to the presence of IBS paste which fills the volume of the scaffold so that it can be stronger in supporting the load so that a greater maximum force was obtained. This increase indicates that more IBS paste enters the scaffold, thereby increasing its bending strength.

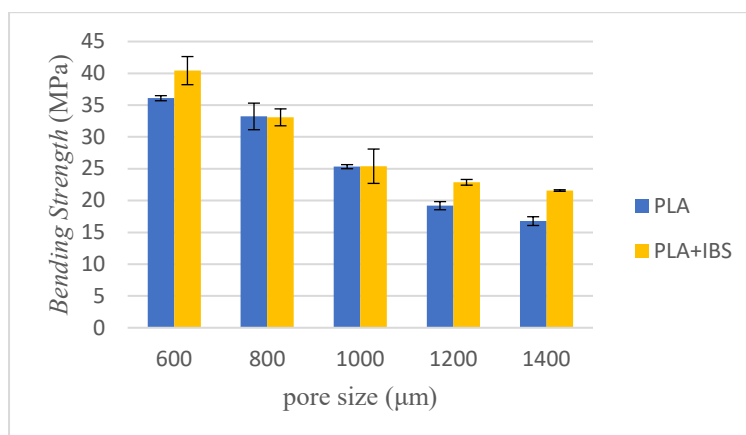


Figure 6. The graph of the compressive strength test results of PLA and PLA+IBS scaffolds

3.7 Streptomycin Release Test

Test using a UV-Visible spectrophotometer was conducted to determine the potential release of streptomycin from the scaffold. Scaffolds with variations of five pore sizes that have been injected with IBS paste were tested for each sample. The wavelength to observe the absorption of the

streptomycin is around 272-274 nm [35]. Before testing the scaffold, a standard curve was made by testing several concentrations of streptomycin using a UV-Vis spectrophotometer. The concentration of streptomycin used was 1-5% in 10 ml of PBS. Based on this test, the absorbance data were obtained from each solution concentration (Figure 7a).

The value of each absorbance peak was used to create a linear standard curve, and a relationship was found between the concentration of streptomycin tested and the absorbance value. The relationship between absorbance value as y-axis and streptomycin concentration as x-axis is depicted in Cartesian diagram with linear regression equation [36]. The standard curve for streptomycin release is presented in Figure 7b. The regression equation is obtained:

$$y = 0.4608 x + 0.086 \quad (3)$$

So that the equation can be made to find the concentration of the drug released. Equation 4 defines the concentration of streptomycin released from the scaffold as the absorbance value minus the correction factor which is then divided by the gradient graph in Figure 7b. In mathematical form, Equation 4 can be written:

$$\text{concentration} = \frac{(\text{absorbance} - 0.086)}{0.4608} \quad (4)$$

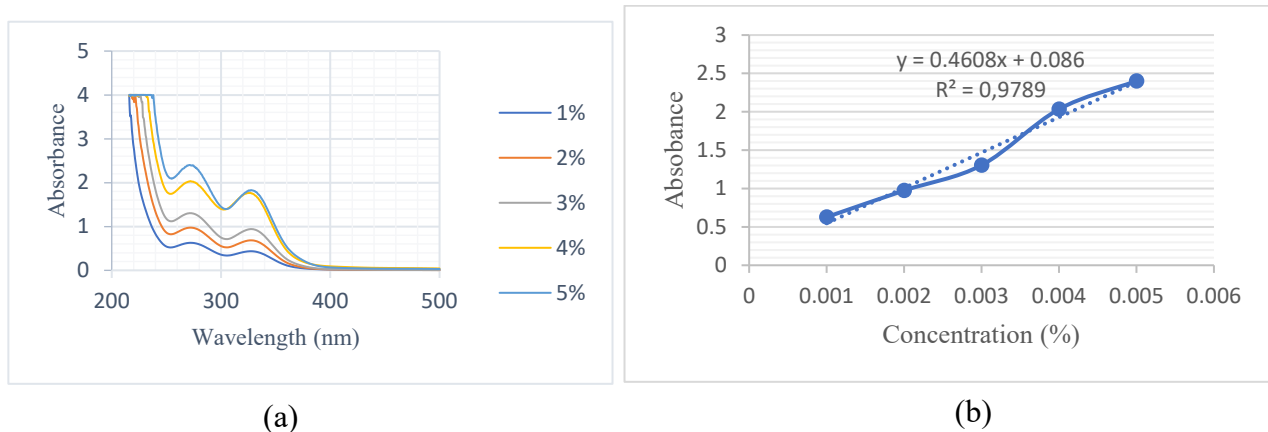


Figure 7. (a) Absorbance of UV-Vis calibration solution, (b) standard curve of streptomycin concentration

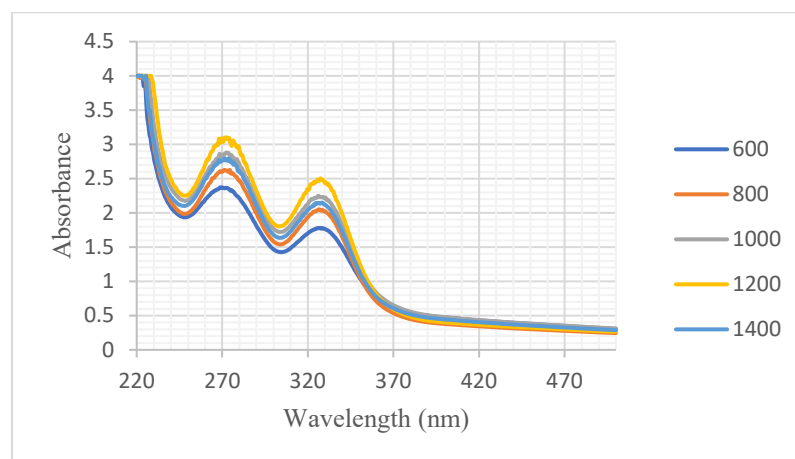


Figure 8. UV-Vis absorbance results for streptomycin released from 5 variations of IBS paste scaffold pore size

The graph of peak absorbance of each scaffold injected with IBS paste can be seen in Figure 8. The absorbance results for each scaffold with variations in pore size were then substituted into the concentration calculation (Eq.2) to obtain the percentage of streptomycin released. Concentration of released streptomycin data can be seen in Table 2.

Table 2. Result of released streptomycin concentration

Pore size of <i>scaffold</i> (μm)	Absorbance	Concentration of released streptomycin (%)
600	2.364	4.944
800	2.625	5.510
1000	2.881	6.066
1200	3.103	6.547
1400	2.793	5.875

Based on the results above, the concentration of released streptomycin for all pore sizes ranged from 4.944% to 6.547%. Referring to research conducted by [4], the released streptomycin concentration of 0.6% was able to kill bacteria with an inhibition zone of 28-33 mm from the initial diameter of 9 mm. The results of this study indicate that the percentage of drug released was able to kill the *Mycobacterium tuberculosis*, thus proving that 3D printing scaffold combined with IBS paste can be used as a method of treating tuberculosis.

The results of this study have limitations, especially in the pore design and the properties studied are only limited to the pore design in the form of a truncated hexahedron. In fact, there are many forms of pore design that can be varied and tested for various physical properties, degradation rates, and all of them have not been reported.

In addition, this research can be developed by testing other characteristics of the 3D printing scaffold after the injection of IBS paste through in vitro tests, namely the MTT assay test and anti-TB test. Another test on the characteristics of the scaffold, namely the in vivo test, can be conducted to determine the ability of the scaffold as a substitute for human bone.

4. Conclusion

Fabrication of 3D printing scaffold has been conducted with the design of truncated hexahedron. Hydroxyapatite combined with gelatin, HPMC, and streptomycin, then injected into the 3D printing scaffold as a means of drug carrier and a method of treating spinal tuberculosis. The results show that the scaffold has interconnectivity between pores. SEM test results showed that the IBS paste had been set in the scaffold and micropores were formed. Based on the results of the EDX test, the Ca/P ratio was 1.90 which was close to the hydroxyapatite ratio. Based on the value of the Ca/P ratio, it has been proven the presence of HA in the IBS paste. Mechanical tests showed that the scaffold for all pore sizes had a compressive strength of 1.49-3.97 MPa and increased to 3.45-4.77 MPa after IBS injection. Then the bending test showed that the scaffold had a bending strength of 16.76-36.09 MPa and increased to 21.57-40.36 MPa after being injected with IBS. The drug release test showed that the 3D printing scaffold could release 4.944%-6.547% of streptomycin which had met the percentage of drug release that was able to kill *Mycobacterium tuberculosis*. It can be concluded that 3D printing scaffold combined with IBS paste can be applied as a drug carrier as well as a method of healing spinal tuberculosis. This research can be developed by testing other characteristics of the 3D printing scaffold after injection of IBS paste through in vitro and in vivo tests to determine the ability of the scaffold as a tissue engineering bone replacement.

Acknowledgments

This work was supported by Universitas Airlangga with research funding [Decree number 8/E1/KPT/2021 and Contract agreement number 4/E1/KP.PTNBH/2021 and 677/UN3.15/PT/2021].

References

- [1] World Health Organization (WHO) global tuberculosis report accessed from <https://www.who.int/publications/i/item/9789240013131>. accessed on 8th May 2022 at 09.20 PM.
- [2] TB Indonesia accessed from <https://tbindonesia.or.id/pustaka-tbc/dashboard-tb/> accessed on 12nd July 2022 at 09.02 PM.
- [3] Liang, X., Weiyang, Z., Zhengxue, Q., Xiao-Ji, L., and Dian-Ming, J. One-Stage Posterior Debridement with Transverse Process Strut as Bone Graft in The Surgical Treatment of Single-Segment Thoracic Tuberculosis. *Medicine*. 2019. 98 (47). https://journals.lww.com/md-journal/Fulltext/2019/11220/One_stage_posterior_debridement_with_transverse.50.aspx
- [4] Hikmawati, D., Maulida, H.N., Putra, A.P., Budiatin, A.S., Syahrom. Synthesis and Characterization of Nanohydroxyapatite-Gelatin Composite with Streptomycin as Antituberculosis Injectable Bone Substitute. *International Journal of Biomaterials*, 2019, Vol. 2019. <https://www.hindawi.com/journals/ijbm/2019/7179243/>
- [5] Li, Y., Yu, B., Ai, F., Wu, C., Zhou, K., Cao, C., Li, W., Characterization and evaluation of polycaprolactone/hydroxyapatite composite scaffolds with extra surface morphology by cryogenic printing for bone tissue engineering. *Materials & Design*, 2021, (205):109712. <https://www.sciencedirect.com/science/article/pii/S0264127521002641?via%3Dihub>
- [6] Sears, N.A.; Seshadri, D.R.; Dhavalikar, P.S.; Cosgriff-Hernandez, E. A review of three-dimensional printing in tissue engineering. *Tissue Eng. Part B*, 2016, Rev. 22, 298–310. <https://www.liebertpub.com/doi/10.1089/ten.teb.2015.0464>
- [7] Vyas, C.; Zhang, J.; Øvrebø, Ø.; Huang, B.; Roberts, I.; Setty, M.; Allardyce, B.; Haugen, H.; Rajkhowa, R.; Bartolo, P. 3D printing of silk microparticle reinforced polycaprolactone scaffolds for tissue engineering applications. *Mater. Sci. Eng. C*. 2020, 118, 111433. <https://www.sciencedirect.com/science/article/pii/S0928493120333518?via%3Dihub>
- [8] Song, X.; Tetik, H.; Jirakittsonthon, T.; Parandoush, P.; Yang, G.; Lee, D.; Ryu, S.; Lei, S.; Weiss, M.L.; Lin, D. Biomimetic 3D printing of hierarchical and interconnected porous hydroxyapatite structures with high mechanical strength for bone cell culture. *Adv. Eng. Mater.* 2019, 21, 1800678. <https://doi.org/10.1002/adem.201800678>
- [9] Wichniarek, R.; Hamrol, A.; Kuczko, W.; Górski, F.; Rogalewicz, M. ABS filament moisture compensation possibilities in the FDM process. *CIRP J. Manuf. Sci. Technol.* 2021, 35, 550–559. <https://doi.org/10.1016/j.cirpj.2021.08.011>
- [10] Anitha, R.; Arunachalam, S.; Radhakrishnan, P. Critical parameters influencing the quality of prototypes in fused deposition modelling. *J. Mater. Process. Technol.* 2001, 118, 385–388. [https://doi.org/10.1016/S0924-0136\(01\)00980-3](https://doi.org/10.1016/S0924-0136(01)00980-3)
- [11] Daly, A.C.; Freeman, F.E.; Gonzalez-Fernandez, T.; Critchley, S.E.; Nulty, J.; Kelly, D.J. 3D bioprinting for cartilage and osteochondral tissue engineering. *Adv. Healthc. Mater.* 2017, 6, 1700298. <https://onlinelibrary.wiley.com/doi/10.1002/adhm.201700298>
- [12] Park, S., Kim, J.E., Han, J., Jeong, S., Lim, J.W., Lee, M.C., Son, H., Kim, H.B., Choung, Y.H., Seonwoo, H., Chung, J.H., Jang, K.J., 3D-Printed Poly(ε Caprolactone)/Hydroxyapatite Scaffolds Modified with Alkaline Hydrolysis Enhance Osteogenesis In Vitro. *Polymers*, 2021, (13):257. <https://www.mdpi.com/2073-4360/13/2/257>
- [13] Hosseinnejad, F., Imani Fooladi, A. A., Hafezi, F., Mafi, S. M., Amiri, A., & Nourani, M. R. Modelling and Tissue Engineering of Three Layers of Calvarial Bone as a Biomimetic Scaffold. *Journal of Biomimetics, Biomaterials and Tissue Engineering*, 2012, 15, 37–53. <https://doi.org/10.4028/www.scientific.net/jbbte.15.37>

- [14] Mohamed, R.M.; Yusoh, K. A review on the recent research of polycaprolactone (PCL). In *Proceedings of the Advanced Materials Research*; Trans Tech Publications Ltd.: Baech, Switzerland, 2016; pp. 249–255. <https://doi.org/10.3390/polym13020257>
- [15] Camargo, J.C.; Machado, Á.R.; Almeida, E.C.; Silva, E.F.M.S. Mechanical properties of PLA graphene filament for FDM 3D printing. *Int. J. Adv. Manuf. Technol.* 2019, *103*, 2423–2443. <https://doi.org/10.1007/s00170-019-03532-5>
- [16] Pascual-González, C., Vega, J. de la, Thompson, C. Fernández-Blázquez, J.P., Herráez-Molinero, D., Biurrún, I. Lizarralde, N., Sánchez del Río, J., González, C., Llorca, J., Processing and mechanical properties of novel biodegradable poly-lactic acid/Zn 3D printed scaffolds for application in tissue regeneration. *Journal of the Mechanical Behavior of Biomedical Materials*, 2022, *132*: 105290. <https://doi.org/10.1016/j.jmbbm.2022.105290>
- [17] Lee, S. H., Zhou, W. Y., Wang, M., Cheung, W. L., & Ip, W. Y. Selective Laser Sintering of Poly(L-Lactide) Porous Scaffolds for Bone Tissue Engineering. *Journal of Biomimetics, Biomaterials and Tissue Engineering*, 2008, *1*, 81–89. <https://doi.org/10.4028/www.scientific.net/jbbte.1.81>
- [18] Karimi, A., Mole, N., Pepelnjak, T., Numerical Investigation of the Cycling Loading Behavior of 3D-Printed Poly-Lactic Acid (PLA) Cylindrical Lightweight Samples during Compression Testing. *Appl. Sci.* 2022, *12*:8018. <https://doi.org/10.3390/app12168018>
- [19] Ostafinska, A.; Fortelný, I.; Hodan, J.; Krejčíková, S.; Nevoralová, M.; Kredatusová, J.; Kruliš, Z.; Kotek, J.; Šlouf, M. Strong synergistic effects in PLA/PCL blends: Impact of PLA matrix viscosity. *J. Mech. Behav. Biomed. Mater.* 2017, *69*, 229–241. <https://doi.org/10.1016/j.jmbbm.2017.01.015>
- [20] Maulida, H.N., Hikmawati, D., Budiatin, A.S., Injectable Bone Substitute Paste Based on Hydroxyapatite, Gelatin, and Streptomycin for Spinal Tuberculosis. *Journal of SCRTE*, 2019, *3* (2). <https://e-journal.unair.ac.id/JSCRTE/article/view/20133>
- [21] Shavandi, A., Bekhit, A. E.-D. A., Sun, Z. F., & Ali, A. A Review of Synthesis Methods, Properties and Use of Hydroxyapatite as a Substitute of Bone. *Journal of Biomimetics, Biomaterials and Biomedical Engineering*, 2015, *25*, 98–117. <https://doi.org/10.4028/www.scientific.net/jbbbe.25.98>
- [22] Liang, L.F., Han, X.Y., Yan, X.C., Weng, J., Reinforcing of Porous Hydroxyapatite Ceramics with Hydroxyapatite Fibres for Enhanced Bone Tissue Engineering. *Journal of Biomimetics, Biomaterials and Tissue Engineering*, 2011, *10*, 67–73. <https://doi.org/10.4028/www.scientific.net/jbbte.10.67>
- [23] Gomez-Lizarraga, K.K.; Flores-Morales, C.; Del Prado-Audelo, M.L.; Alvarez-Perez, M.A.; Pina-Barba, M.C.; Escobedo, C. Polycaprolactone- and polycaprolactone/ceramic-based 3D-bioploted porous scaffolds for bone regeneration: A comparative study. *Mater. Sci. Eng. C Mater. Biol. Appl.* 2017, *79*, 326–335. <https://doi.org/10.1016/j.msec.2017.05.003>
- [24] Szczes, A.; Holysz, L.; Chibowski, E. Synthesis of hydroxyapatite for biomedical applications. *Adv. Colloid. Interface Sci.* 2017, *249*, 321–330. <https://doi.org/10.1016/j.cis.2017.04.007>
- [25] Kim CG, Han KS, Lee S, Kim MC, Kim SY, Nah J. Fabrication of biocompatible polycaprolactone-hydroxyapatite composite filaments for the FDM 3D printing of bone scaffolds. *Appl Sci* 2021;11:6351. <https://www.mdpi.com/2076-3417/11/14/6351>

- [26] You, B.C., Meng, C.E., Nasir, N.F.M., Tarmizi, E.Z.M., Fhan, K.S., Kheng, E.S, Majid, M.S.A., Jamir, M.R.M. Dielectric and biodegradation properties of biodegradable nano-hydroxyapatite/starch bone scaffold. *Journal of materials research and technology*. 2022, 18:3215-3226. <https://doi.org/10.1016/j.jmrt.2022.04.014>
- [27] Putra, A. P., Rahmah, A. A., Fitriana, N., Rohim, S. A., Jannah, M., & Hikmawati, D. The Effect of Glutaraldehyde on Hydroxyapatite-Gelatin Composite with Addition of Alendronate for Bone Filler Application. *Journal of Biomimetics, Biomaterials and Biomedical Engineering*, 2018, 37, 107–116. <https://doi.org/10.4028/www.scientific.net/jbbbe.37.107>
- [28] Asgari, B., Azami, M., Amiri, A., Imani Fooladi, A. A., & Nourani, M. R. Bone Scaffold Biomimetics Based on Gelatin Hydrogel Mineralization. *Journal of Biomimetics, Biomaterials and Tissue Engineering*, 2013, 17, 59–69. <https://doi.org/10.4028/www.scientific.net/jbbte.17.59>
- [29] C. Chang, C. Hu, Y. Chang. Two-stage revision arthroplasty for Mycobacterium Tuberculosis periprosthetic joint infection: an outcome analysis, *PLoS ONE*, 2018, vol. 13, no. 9, Article ID e0203585, pp. 1–13,. <https://doi.org/10.1371/journal.pone.0203585>
- [30] Zimmerling, A., Yazdanpanah, Z., Cooper, D.M.L., Johnston, J.D., Chen, X., 3D printing PCL/nHA bone scaffolds: exploring the influence of material synthesis techniques. *Biomaterials Research*, 2021, (25):3. <https://biomaterialsres.biomedcentral.com/articles/10.1186/s40824-021-00204-y>
- [31] Liu L, Liu J, Wang M, Min S, Cai Y, Zhu L, Yao J. Preparation and characterization of nano hydroxyapatite/silk fibroin porous scaffolds. *Biomater Sci*. 2012;325–338 doi:<https://doi.org/10.1163/156856208783721010>
- [32] Zhao, H., Li, L., Ding, S., Liu, C., and Ai, J. Effect Of Porous Structure and Pore Size on Mechanical Strength of 3D-Printed Comby Scaffolds. *Materials Letters*. 2018. 223: 21–24. <http://dx.doi.org/10.1016/j.matlet.2018.03.205>
- [33] Warastuti, Y., & Abbas B., Synthesis and Characterization of Hydroxyapatite-Based Irradiated Injectable Bone Substitute Paste. *Journal of Isotope and Radiation Applications*, 2011, 7(2), 73-82. <https://adoc.pub/queue/synthesis-and-characterization-of-irradiated-injectable-bone.html>
- [34] Kurutz, M., M. Galos, P. Varga, B. Fornet, Regional Age-And Sex- Related Compressive Strength Parameters of Human Lumbar Vertebrae in Osteoporosis, Portugal: *8th Computer Methods In Biomechanics And Biomedical Engineering Symposium*. 2018 <https://doi.org/10.2147%2Fjmdh.s4103>
- [35] Wardhani, I.F., Samudra, R.M.R., Katherine., Hikmawati, D., In vitro study of Nano Hydroxyapatite/Streptomycin-Gelatin-Based Injectable Bone Substitute Associated- 3D printed Bone Scaffold for Spinal Tuberculosis Case. *Journal of Physics: Conference Series*. 2020, <https://iopscience.iop.org/article/10.1088/1742-6596/1445/1/012003>
- [36] J. Dong, S. Zhang, J. Ma., Preparation, characterization, and in vitro cytotoxicity evaluation of a novel anti-tuberculosis reconstruction implant, *PLoS ONE*, vol. 9, no. 4, Article ID e94937, pp. 1–10, 2014. <https://doi.org/10.1371/journal.pone.0094937>